Ain Shams University

Faculty of Science

Geophysics Department

Multi-Dimensional Seismic Attributes and Density Models of the Hydrocarbon Plays Inferred from Seismic Reflection and Bouguer Gravity Data at the Southern Region of West El Qantara In the Nile Delta Basin, Northern Egypt

A Thesis submitted in Partial Fulfillment of the Requirements for the Master Degree of Science in Geophysics

By

Amir Abdel Azim Ibrahim El Motany

(B. Sc. in Geophysics, Faculty of Science, Ain Shams University, 1995)

To

Geophysics Department

Faculty of Science

Ain Shams University

Supervised by

Prof. Dr. Abdel Naser Mohamed A. Helal
Professor of Geophysics – Geophysics Department – Faculty of Science – Ain Shams University

Dr. Karam Samir Ibrahim Farag
Assis. Professor of Geophysics – Geophysics Department – Faculty of Science – Ain Shams University

Cairo – 2019

Note

The present thesis is submitted to Faculty of Science, Ain Shams University in partial fulfillment for the requirements of the Master degree of Science in Geophysics.

Beside the research work materialized in this thesis, the candidate has attended ten post-graduate courses for one year in the following topics:

1- Geophysical field measurements.

2- Numerical analysis and computer programming.

3- Elastic wave theory.

4- Seismic data acquisition.

5- Seismic data processing.

6- Seismic data interpretation.

7- Earthquake seismology.

8- Engineering seismology.

9- Deep seismic sounding.

10- Structure of the earth.

He successfully passed the final examinations in these courses.

In fulfillment of the language requirement of the degree, he also passed the final examination of a course in the English language.

Head of Geophysics Department

Prof. Dr. Samy Hamed

ACKNOWLEDGEMENTS

First and foremost, I would like to thank Allah, whose brought to me all the best during my life.

I would like to offer my sincere gratitude to my supervisor, **Prof. Dr**. **Abdel Naser Mohamed Helal**, who has supported me till the end with his patience, knowledge, and giving me the opportunity to be a creative researcher. The completeness of my Master's degree is indebted to his encouragement and effort and I can say without him this thesis, too, would not have been completed or written.

I would like to express my particular gratitude and deep appreciation to **Dr. Karam Samir Ibrahim Farag** for his excellent guidance and advice throughout my research.

I would like to thank the **Department of Geophysics** in Ain Shams University and everyone who has offered advises or any suggestion and provided support when it was needed.

I would like to thank the **Egyptian General Petroleum Corporation** (E.G.P.C.) and **Dana Gas** Company for providing the data set, and their contribution in the research.

I would be honor to dedicate this work to **my parents**. The two persons who have given me the tools of life and the manners of soul which they always are necessary for making me who I am standing

Finally, I would like to express my deepest gratitude to my wife, brothers and sisters for their enthusiastic support, and for their prayers.

ABSTRACT

The Nile Delta Basin is the most significant gas source province in Egypt and one of the most promising areas for future petroleum exploration in North-Eastern Africa. The present area of study is a part of the South West of El Qantara in the northern part the Nile Delta basin of Egypt. It is located between latitudes 30° 54' 00" and 31° 00' 00" N and longitudes 31° 46' 00" and 32° 09' 00" E.

The current study is mainly devoted to integrate between the multi-dimensional geo-seismic and density models that obtained from the gravity data analysis for the purpose of interrelation of both the shallow-seated (mainly sedimentary) with deep-seated (mainly basement) structures. This can help imaging such older and deeper plays (structural reservoirs) in the area.

A basement relief map was constructed after the application of several geophysical filters had applied on the Bouguer gravity map of the study area. This map elucidated the major tectonic trends in the investigated area and displayed the basement topography distribution which constitutes the input data for the density modeling.

In addition, the application of the seismic attributes enhanced the 3D seismic interpretation process by adding the small stratigraphic and structural elements and providing more details on the depositional features which cannot be seen easily, this in turn characterizing the intruded reservoir clearly. Possible hydrocarbon traps were identified in the studied area, which need more detailed geological work to minimize the exploration risk.

Keywords: *Bouguer gravity, Residual gravity, regional gravity, 3D Seismic Interpretation, 3D Seismic Attributes, Variance, Amplitude Extraction, and West El Qantara, Egypt*

LIST OF CONTENTS

ACKNOWLEDGEMENTS II
ABSTRACT III
LIST OF CONTENTS IV
LIST OF FIGURES VII
LIST OF TABELS XII
LIST OF ACRONYMS XIII

CHAPTER 1 1
INTRODUCTION 1
1.1 General Preface 1
1.2 The Exploration History of the Study Area 2
1.3 Previous Geological and Geophysical Work 5
1.4 The Aim of this Work 7

CHAPTER 2 11
GEOLOGICAL SETTING 11
2.1 General Overview 11
2.2. The Stratigraphic Framework 13
2.2.1. Basement Rocks 14
2.2.2. Paleozoic 14
2.2.3. Mesozoic Period 14
(i) Triassic Rocks 15
(ii) Jurassic Rocks 15
(iii) Cretaceous Rocks 15
2.2.4. Cenozoic Period 16
2.2.4.1. Paleogene 16
2.2.4.1.1. Paleocene Rocks 16
2.2.4.1.2. Eocene Rocks 16
2.2.4.1.3. Oligocene Rocks 16
2.2.4.2. Neogene 17
2.2.4.2.1 Miocene Rocks 17
(i) Qantara Formation (Early Miocene) 17

(ii) Sidi Salim Formation (Middle Miocene) 18
(iii) Qawasim Formation (Late Miocene) 19
(iv) Abu Madi Formation (Late Miocene) 20
2.2.4.2.2. Pliocene Rocks 21
(i) Kafr El Sheikh Formation (Early - Middle Pliocene) 21
(ii) El Wastani Formation (Late Pliocene) 21
2.2.4.3. Pleistocene (Holocene Rocks) 22
(i) Mit Ghamr Formation (Late Pliocene-Holocene) 22
(ii) Bilqas Formation 22
2.3. Structural Frame Work 22
2.4. Geological Traps 27
2.5. Petroleum System 29
2.5.1. Source Rocks 30
2.5.2. Reservoir Rocks 30
2.5.3. Cap Rocks 32
2.5.4. Maturation 32
2.5.5. Petroleum Occurrences 32

CHAPTER 3 34
SEISMIC INTERPRETATION 34
3.1. Previous Seismic Investigations in the Study Area 34
3.2. Seismic Data Overview 35
3.2.1. Acquisition Parameters 36
3.2.2 Seismic Processing 41
3.3. Well Logging Data 45
3.4. Well to Seismic Tie (Synthetic Seismogram) 46
3.5. Seismic Interpretation 50
3.5.1. The Identification of the Seismic Horizons 52
(i) Late Pliocene Boundary 53
(ii) Middle Pliocene Boundary 54
(iii) Late Miocene Boundary 55
(iv) Oligocene Boundary 56
(v) Eocene Boundary 57
3.5.2. The Main Structural Features 58
(i) Normal faults 59
(ii) Regional Faults 59

(iii) Fault Blocks 60
(iv) Rollover Anticlines 60
(v) Unconformity Surface 61
(vi) Channels 61
3.5.3. Depth Maps of the Boundaries 64
3.6. Seismic Attributes 68
3.6.1. The Root Main Square (RMS) Attributes. 68
3.6.2. The Variance Attributes 76
3.7. The 3D Structural Modeling 81

CHAPTER 4 84
Gravity Data Interpretation 84
4.1 Introduction 84
4.2. Bouguer Gravity Data 86
4.3 Gravity Data Filtering Techniques 88
4.3.1. Power Spectrum Analysis 90
4.3.2 Gravity Anomaly Separation 92
4.3.3 Basic gradients 94
4.3.3.1 Horizontal Gradient 96
4.3.3.2. Vertical Derivative Transformation 100
4.3.3.3. Local Phase or Tilt Derivative (Θ or TDR) 102
4.3.4 Vertical Continuation Transformation 103
4.4. 3-D Euler Deconvolution 107
4.5 Gravity Data Modeling 113
4.5.1 3D Gravity Modeling 113
4.5.2 2D Gravity Modeling 116
4.6. The Fault Tectonic Trends 120
4.7. The Regional Comparison of the Gravity Maps 120

CHAPTER 5 123
DISCUSSION AND CONCLUSION 123

REFERENCES 130

LIST OF FIGUERS

Fig. (1.1): Location map of the study area of in the Nile Delta of Egypt. 1

Fig. (1.2): The Gas and condensate discoveries in the W. Manzala and W. El Qantara blocks, after (Dana Gas, 2009). 3

Fig. (1.3): The location map of the study area including wells. 8

Fig. (2.1): Schematic cross section based on regional seismic profiles across the Nile Delta and the Mediterranean showing major petroleum plays. 12

Fig. (2.2): The Generalized Stratigraphic Section of the Nile Delta, modified after (Schlumberger, 1984). 13

Fig. (2.3): Showing the depositional environment of Qantara formation, after (Haq et al., 1987). 18

Fig. (2.4): Early Miocene facies and thicknesses in the Cairo-Suez District, after (Harms and Wray, 1990). 19

Fig. (2.5): Main subsurface structures of the Nile Delta region, after Sestini (1989). 23

Fig. (2.6): Northern Egypt Fault Pattern and Tectonic Setting, after (Meshref, 1990) 25

Fig. (2.7): The Nile Delta Tectonic Setting, after (Sestini, 1989). 26

Fig. (2.8):The major fault tectonic trends and the recent earthquake epicenters locations at the Nile Delta of Egypt, after (Saleh, 2013). 28

Fig. (2.9): Nile Delta Onshore Play Model 29

Fig. (2.10): Nile Delta and Mediterranean Regional map showing different reservoir play type discoveries, after (Ahmed, 2002). 31

Fig. (3.1): Base map with old 2d and the recent 3D seismic program. 36

Fig. (3.2): The Pelton Shot Pro Dynamite firing system. 37

Fig (3.3): Normal Array (Geophone Layout), after (Dana Gas, 2009). 38

Fig. (3.4): Cross Line Array (Geophone Layout), after (Dana Gas, 2009). 38

Fig. (3.5): Shot after anomalous amplitude attenuation AAA. 44

Fig. (3.6): An example of stacking before the Fk filter. 44

Fig. (3.7): An example of stacking after the application of Fk dip filter (+/-) 25. 45

Fig. (3.8): Synthetic seismogram of Sama-1 well with correlation factor 0.7 46

Fig (3.9):N-S Inline seismic line # 512125 showing the tie between synthetic and the seismic wavelets along Sama-1 well. 49

Fig. (3.10): E-W Cross-line seismic line #110425 showing the tie between synthetic and the seismic line along Sama-1 well. 50

Fig. (3.11):3D visualization of a block model shows the observed stratigraphic boundaries in the study area. 53

Fig. (3.12): The TWT time map of El Wastani Fm. 55

Fig. (3.13): The TWT time map of Kafr El Sheikh Fm. 55

Fig. (3.14): The TWT time map of Abu Madi fm (Late Miocene). 56

Fig. (3.15): The TWT time map of the top Oligocene boundary. 57

Fig. (3.16): The TWT time map of the Eocene boundary. 58

Fig. (3.17): Base map showing the location of two seismic lines A& B. 59

Fig.(3.18):Line (A) showing the structures and geological features in the study area. 62

Fig.(3.19):Line (B) showing the structures and geological features in the study area. 63

Fig. (3.20): The depth map of El Wastani formation 65

Fig. (3.21): The depth map of Kafr El Sheikh formation 66

Fig. (3.22): The Structural depth map of Abu Madi formation 66

Fig. (3.23): The Structural depth map of the Oligocene Boundary 67

Fig. (3.24): The Structural depth map of the Eocene Boundary 67

Fig. (3.25): The RMS attribute slice map above the El Wastani formation by extraction window of 80 ms 69

Fig. (3.26): The RMS Amplitude map of the Eastern part of the study area and the seismic Section A which represent the stacked channels. 70

Fig. (3.27): (a) RMS Amplitude map of the Western part of the study, (b) Seismic Section B showing the isolated Meander channels, (c) RMS Amplitude map with transparency applied. 71

Fig. (3.28): (a) RMS amplitude extraction from below KES level 100: 200 ms, (b) RMS amplitude extraction from below KES level 200: 300 ms, (c) Seismic Section passing through RMS anomalies. 73

Fig. (3.29): RMS amplitude extraction from AM level to 80 ms below 75

Fig. (3.30): RMS amplitude extraction from Oligocene level to 40 ms below 76

Fig. (3.31): RMS amplitude extraction from Eocene level to 40 ms below 76

Fig. (3.32): The Variance time slice at 500 ms 78

Fig. (3.33): The Variance time slice at 750 ms 78

Fig. (3.34):a) Variance time slice at 1500 ms, (b) Interpreted variance time slice at 1500 ms 80

Fig. (3.35): The Variance time slice at 2000 ms. 81

Fig. (3.36): The Variance time slice at 2500 ms 81

Fig. (3.37): An Oblique view displays the four depth-surfaces Kafer El Sheikh, Abu Madi, the Oligocene and the Miocene from top to bottom 83

Fig. (4.1): The Bouguer gravity map of the study area, after (G.P. C., 1985). 87

Fig. (4.2): Radially averaged power spectrum and depth estimate of the Bouguer gravity map. 91

Fig. (4.3): The regional gravity map of the study area. 93

Fig. (4.4): Color shaded residual gravity map of the study area. 94

Fig. (4.5): Color shaded map of the horizontal gradient (in x-direction) of the residual gravity map of the study 97

area.

Fig. (4.6): Color shaded map of the horizontal gradient (in y-direction) of the residual gravity map of the study area. 97

Fig. (4.7): Color shaded map of the second horizontal gradient (in x-direction) of the residual gravity map of the study area. 98

Fig. (4.8): Color shaded map of the second horizontal gradient (in y-direction) of the residual gravity map of the study area. 98

Fig. (4.9): Color shaded map of the total horizontal gradient of the residual gravity map of the study area. 99

Fig. (4.10): Color shaded map of the maximum horizontal gradient amplitude of the residual gravity map of the study area 99

Fig. (4.11): The first Vertical Derivative map after applying the upward continuation filter for noise removal. 101

Fig. (4.12): The second Vertical Derivative map after applying the upward continuation filter for noise removal. 101

Fig. (4.13): Color shaded map of the tilt derivative of the residual gravity map of the study area 103

Fig. (4.14): Downward continuation map at the depth level 1 Km. 104

Fig. (4.15): Downward continuation map at the depth level 2 Km. 105

Fig. (4.16): Downward continuation map at the depth level 3 Km. 105

Fig. (4.17): Downward continuation map at the depth level 4 Km. 106

Fig. (4.18): Downward continuation map at the depth level 5 Km. 106

Fig. (4.19): (a) Euler solutions (SI= 0), (b) Euler solutions superimposed on the Bouguer gravity map. 109

Fig. (4.20): (a) Euler solutions (SI= 0), (b) Euler solutions superimposed on the residual gravity map. 111

Fig. (4.21): Digital Elevation Model (DEM) of the study area compiled from SRTM (Shuttle Radar Topography Mission) [With Spatial Resolution = 90 m]. 114

Fig. (4.22): The observed gravity map of the study area. 114

Fig. (4.23): The Calculate gravity map of the study area. 115

Fig. (4.24): The error model percentage map of the study area. 115

Fig. (4.25): The basement relief map of the study area. 116

Fig. (4.26): The location of the three selected profiles on the basement relief map of the study area. 117

Fig. (4.27): The depth Model along profile (1), the density of sedimentary sequence D=2.43 gm/cc, while for the basement rocks D= 2.75 gm/cc). 118

Fig. (4.28): The depth Model along profile (2), the density of sedimentary sequence D=2.41 gm/cc, while for the basement rocks D= 2.75 gm/cc). 118

Fig. (4.29): The depth Model along profile (3), the density of sedimentary sequence D=2.40 gm/cc, while for the basement rocks D= 2.75 gm/cc). 119

Fig. (4.30): The summation Azimuth fault tectonic trends deducted from the observed Bouguer gravity map of the study area. 120

Fig. (4.31): The top basement map overlaid by the main fault trends, modified after (Garfunkel and Bartov, 1977); (Garfunkel, 1981); (Ben-Avraham, 1985); (Brew et al., 1999); and (Abdel Aal et al., 2001); 122

LIST OF TABELS

Table (3.1): The Recording Parameters of the Seismic Data 39
Table (3.2): The Recording Patch Parameters. 39
Table (3.3): The Receiving Parameters. 40
Table (3.4): The Source Parameters. 40
Table (3.5): The Spreading Geometry. 41
Table (3.6): The Receiver Layout Parameters of the Normal Array. 41
Table (3.7): The Parameters of some Applied Filters on the Seismic Data. 43
Table (4.1): Structure Index (SI) for simple models of gravity field's,(Geosoft 2015). 107

LIST OF ACRONYMS

AI Acoustic Impedance

bcf	Billion cubic feet
CDP	Common Depth Point
DEM	Digital Elevation Model
DHI	Direct Hydrocarbon Indicator
ft	Feet
FFT	Fast Fourier Transform
gu	Gravity Unit “Gal”
GDT	Gas Down To
GWC	Gas Water Contact
ILN	In Line
KES	Kafr El Sheikh formation - Pliocene
MMscfd	Million Standard Cubic Feet per Day
ms	Millisecond
NMO	Normal Move Out
OWT	One Way Time
R	Reflectivity
R. C.	Reflection Coefficient
RMS	Root Mean square amplitude extraction
TWT	Two Way Time
VSP	Vertical Seismic Profile
WEM	West El Manzala
WEQ	West El Qantara
XLN	Cross line

CHAPTER 1
INTRODUCTION

1.1 General Preface

The Nile Delta is considered one of the earliest known deltas all over the world. Although its oldest formation, there is a lack of work has been published on the geological evolution of the Nile Delta. The Nile Delta was early described in Herodotus writings in the 5th Century A.C. (Said, 1981). The Nile Delta is illustrated to be an arcuate delta (arc-shaped), as it looks like an irregular triangle, Fig. (1.1).

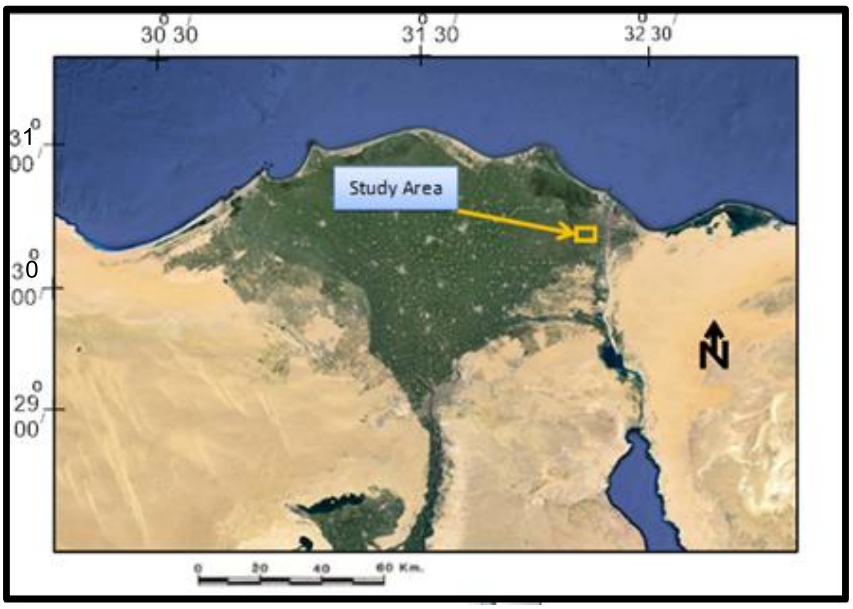

Fig. (1.1): Location map of the study area of in the Nile Delta of Egypt.

The area of the Nile Delta onshore about 25,000 km^2 and it displays an equal amount offshore recording 200 m depth beneath water. The Delta begins approximately 20 Km north of Cairo and extends to the North about